Determination of chemotherapeutic activity *in vivo* by luminescent imaging of luciferase-transfected human tumors

Gisela Caceres[a], Ralitza Zankina[a], XiaoYun Zhu[b], Jin-an Jiao[b], Hing Wong[b], Alex Aller[a] and Peter Andreotti[a,c]

Human DU-145 prostate and MCF-7 breast tumor cell lines were stably transfected with plasmid pcDNA3.1-Luc expressing firefly luciferase. Studies were performed with the transfected cell lines to evaluate luminescent imaging for measuring the efficacy of anti-cancer agents. *In vitro* experiments demonstrated a dose response of both cell lines to topotecan (Hycamtin®) with an IC_{50} of 0.013 μM for MCF-7 Luc cells and 0.002 μM for DU-145 Luc cells. *In vivo* imaging experiments were performed using athymic nude mice inoculated i.p. with 5×10^6 MCF-7 cells or s.c. with 5×10^6 DU-145 cells and then treated with topotecan at 2.5 mg/kg body weight. Tumor progression and regression were monitored for 27 days. Animals inoculated s.c. with DU-145 Luc cells and then treated with topotecan demonstrated significant tumor growth and regression as measured with calipers and luminescent imaging. High correlation was observed between caliper and imaging results. The correlation coefficient was 0.75 for the control untreated group and 0.93 for the topotecan-treated group. Similarly, tumor progression and regression were measurable using luminescent imaging for untreated and topotecan-treated mice inoculated i.p. with MCF-7 Luc cells. These data indicate that luminescent imaging is a useful tool for evaluating anti-cancer drugs *in vivo* and may prove to be particularly useful for the development of novel agents. Luminescent imaging could also be used to locate and harvest residual tumors in drug-treated animals in order to study mechanisms of drug resistance. *Anti-Cancer Drugs* 14:569–574 © 2003 Lippincott Williams & Wilkins.

Anti-Cancer Drugs 2003, **14**:569–574

Keywords: imaging, luciferase, topotecan, tumors

[a]Rumbaugh-Goodwin Institute for Cancer Research, Inc., Plantation, FL, USA, [b]Sunol Molecular Corp., Miramar, FL, USA and [c]Atlantic Scientific Development, Inc., Plantation, FL, USA.

Sponsorship: This work was supported by the Community Foundation of Broward.

Corresponding to P Andreotti, Rumbaugh-Goodwin Institute for Cancer Research, Inc., 1850 NW 69th Avenue, Suite 5, Plantation, FL 33313, USA.
Tel: +1 954 587-9020; fax: +1 954 321-5311;
e-mail: Alex@rgicr.org

Received 24 April 2003 **Revised form accepted** 20 May 2003

Introduction

Pre-clinical research, development and testing of new chemotherapeutic agents requires both *in vitro* and *in vivo* assays systems [1–12]. *In vitro* systems for screening and testing of new agents are generally performed using tumor cell lines and clinical specimens as targets prior to *in vivo* model studies. Pre-clinical *in vivo* studies commonly utilize human tumor xenografts in athymic nude mice. Optimal *in vivo* model systems should allow quantitative analysis of drug activity on primary tumor growth in deep tissues and the progression of metastasis to distant organs [13–22].

Luciferase imaging has been widely used for different *in vitro* and *in vivo* applications, including the study of individual cells [23–25], determining the progression of viral and bacterial infections in mammals [26–30], measuring human tumor growth in animal models [9,31,32], and characterizing metastasis of human cervical tumors [33]. Recent studies have demonstrated the efficacy of using luciferase (Luc)- and green fluorescence protein (GFP)-transfected human tumor cells to study tumor development in experimental animals [31,34–41]. In a previous report, we have demonstrated the use of *in vivo* luminescent imaging to measure luciferase-transfected human breast tumor cells in s.c. and i.p. tumors, and also in deep tissue lesions such as lung and lymph node metastases [9,34].

In this report, we demonstrate the application of *in vivo* luminescence imaging with luciferase-transfected human tumors to study the activity of chemotherapeutic agents against i.p. and s.c. xenografts. Imaging studies were performed using xenografts of luciferase-transfected human prostate carcinoma DU-145 cells and breast adenocarcinoma MCF-7 cells. Topotecan, which binds topoisomerase I required for cell growth and proliferation [42–46], was tested *in vivo* using model systems of DU-145 Luc tumors in male athymic *nu/nu* mice and MCF-7 Luc tumors in female athymic *nu/nu* mice.

Materials and methods

Cell lines

The human mammary adenocarcinoma cell line MCF-7 (HTB-22; ATCC, Rockville, MD) and human prostate carcinoma cell line DU-145 (HTB-81; ATCC) were

0959-4973 © 2003 Lippincott Williams & Wilkins DOI: 10.1097/01.cad.0000086656.37889.23

transfected with the firefly luciferase-expressing vector as previously described [34]. Briefly, cells were transfected with the vector pcDNA3.1-Luc by Lipofectamine Plus (Invitrogen, Carlsbad, CA) according to the manufacturer's protocol. To create pcDNA3.1-Luc, the engineered firefly luciferase gene from the pSP-Luc vector (Promega, Madison, MI) was cloned to pcDNA3.1 (Invitrogen) at *Nhe*I and *Xho*I sites. Stable MCF-7 and DU-145 transfectants that expressed high levels of luciferase were cloned by either limiting dilution or cloning disks (Sigma, St Louis, MO), and selected by Geneticin (Invitrogen), using 2 mg/ml for MCF-7 Luc and 1.5 mg/ml for DU-145 Luc. Clones were screened by the Steady-Glo luciferase assay system (Promega) and a microplate spectrofluorometer (Molecular Devices, Palo Alto, CA). Stable clones were maintained in high glucose DMEM (Invitrogen) containing 10% FBS and 0.5 mg/ml of Geneticin at 37°C in 95% humidity/5% CO_2.

In vitro drug sensitivity

Drug sensitivity assays were performed in quadruplicate based on previously published methods for ATP tumor chemosensitivity testing [10]. Topotecan (Hycamtin®) was dissolved in sterile water to a stock concentration of 1 mg/ml, diluted to 6 μg/ml in cultured medium and then serially diluted 1:4 in opaque, white tissue culture-treated microplates (Corning, Corning, NY) to a final volume of 0.1 ml/well. Cells were resuspended in 3×10^4 cells/ml in DMEM with high glucose (Sigma) containing 10% FBS and 0.5 mg/ml Geneticin; 100 μl of cells were added in each well. Plates were incubated for 4 days at 37°C in 95% humidity/5% CO_2. After incubation, 0.05 ml of 0.1 M HEPES buffer (pH 7.9) containing 50 μg/ml D-luciferin (L-8200; Biosynth, Naperville, IL) was added to each well. After incubation at room temperature for 10 min, the culture microplate was measured in a MPL microplate luminometer (Berthold Detection Systems, Bad Wildbad, Germany) and a NightOwl LB 981 molecular light imager (Berthold Technologies, Bad Wildbad, Germany). Results obtained with the MPL microplate luminometer were calculated as described previously [10] using no inhibition control wells without exogenous drug and maximum inhibition control wells containing ATP inhibitor (ASD). Results for the NightOwl LB 981 molecular light imager were similarly calculated using values obtained with a 5 min luminescent image and the WinLight[32] software.

In vivo imaging and caliper measurement

In vivo imaging studies and caliper measurements were performed using 8- to 10-week-old athymic *nu/nu* mice. Sixteen female mice were inoculated i.p. with 5×10^6 MCF-7 Luc tumor cells in 0.2 ml sterile PBS. Twenty male mice were inoculated s.c. with 5×10^6 DU-145 Luc tumor cells in 0.1 ml sterile PBS and 0.1 ml of Matrigel (BD Biosciences, Bedford, MA). Cell viability was over 95% by Trypan blue exclusion at the time of injection. *In vivo* imaging was performed as previously described [34]. Briefly, animals were injected i.p. with 2.0 mg firefly D-luciferin (Biosynth) in 0.1 ml of sterile PBS, anesthetized with xylazine (3 mg/ml) and ketamine (7 mg/ml) in PBS at 0.12 ml/20 g body weight, and then placed in the NightOwl LB 981 molecular light imager. Imaging was then performed using a two-step process and the WinLight[32] software. First, a black and white photographic image was acquired using a 15-ms exposure. Next, the luminescent image was acquired using a 5-min photon integration period with background subtraction. The luminescent image was processed in software to colorize luminescence intensity, and then overlaid onto the black and white photographic image for presentation.

The volume of the s.c. DU-145 Luc tumors was determined by using a caliper to measure the length, width and height of each tumor in millimeters. This formula, $(L \times W \times H)/2 = \text{mm}^3$, was used to calculate the tumor volume. Tumors were measured, and animals were imaged 1 day prior to drug treatment and once every 4 days thereafter.

Drug treatment

Hycamtin, 4 mg (topotecan hydrochloride; SmithKline Beecham, Research Triangle Park, NC) was resuspended in 0.5 ml. sterile water and diluted with 7.5 ml of PBS to a final concentration of 0.25 mg/ml. An experimental group of 13 mice inoculated with MCF-7 Luc was injected i.p. 4 times every 4 days with 2.5 mg/kg of topotecan, beginning 6 days after tumor inoculation. An experimental group of 10 mice inoculated with DU-145 Luc was injected i.p. 4 times every 4 days with 2.5 mg/kg of topotecan, beginning 4 days after tumor inoculation. Control groups of mice inoculated with MCF-7 Luc or DU-145 Luc were injected with PBS using the same protocol. The weight of mice in the experimental and control groups was monitored to demonstrate that topotecan did not affect the health of the animals.

Statistical analysis

The Kruskal–Wallis test was used to compare experimental groups with control groups. Dunn's multiple comparisons test was used for comparison between the groups. Pearson's correlation was used as required.

Results

Initial *in vitro* studies were performed using both microplate luminometry and luminescent imaging to quantify the activity of topotecan against cultured DU-145 Luc prostate cells and MCF-7 Luc breast cells. Figure 1 shows results obtained when measurements were performed 10 min after adding D-luciferin to cells that were cultured for 4 days with serial dilutions of topotecan. Drug activity against both transfected cell lines was measurable by microplate luminometry and

Fig. 1

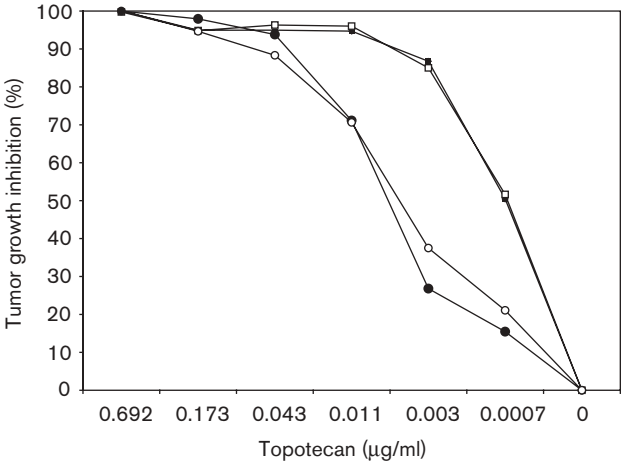

In vitro activity of topotecan against DU-145 Luc prostate and MCF-7 Luc breast cells lines determined by microplate luminometry and luminescent imaging. (○) MCF-7 Luc microplate, (●) MCF-7 Luc imaging, (□) DU-145 Luc microplate and (■) DU-145 Luc imaging.

Fig. 2

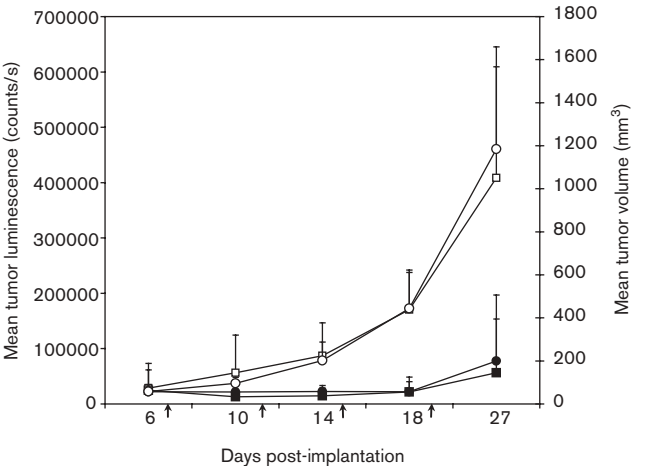

Development of DU-145 solid tumors in male athymic *nu/nu* mice after s.c. inoculation of 5×10^6 cells. Left ordinate shows mean luminescence determined by imaging. Right ordinate shows mean tumor volume determined by caliper. Mice were treated with PBS or topotecan (2.5 mg/kg) on days 7, 11, 15 and 19 after tumor inoculation as shown by arrows. (□) Mean luminescence of control mice treated with PBS, (■) mean luminescence of experimental mice treated with topotecan, (○) mean tumor volume of control mice treated with PBS and (●) mean tumor volume of experimental mice treated with topotecan.

luminescent imaging. Complete inhibition of both cell lines was observed at the highest drug concentration of 0.692 μg/ml. Stronger drug activity was observed for DU-145 Luc with an IC_{50} value of 0.002 μM for both methods compared to an IC_{50} value of 0.013 μM for MCF-7 Luc with both methods.

In vivo studies were performed with athymic male mice inoculated s.c. with DU-145 Luc cells to directly compare caliper measurements with luminescent imaging and quantify tumor growth. As shown in Figure 2, there was no significant difference between results obtained for caliper and imaging measurements for both control mice and mice treated with 2.5 mg/kg of topotecan. Mice treated with topotecan showed significant reduction in tumor growth detectable with both methods, reaching maximum values of approximately 60 mm^3 in volume and 22 000 counts/s by imaging during drug treatment compared with 450 mm^3 in volume and 170 000 counts/s for control mice. The correlation between caliper tumor volume and luminescent imaging for the control group was $r = 0.75$, while the correlation between the two methods for the topotecan-treated group was $r = 0.93$.

Figure 3 shows representative imaging results for control and topotecan-treated mice inoculated s.c. with DU-145 Luc cells. Serial images obtained with control mice showed a progressive increase in both size and overall luminescent intensity of the growing tumor mass. In contrast, topotecan-treated mice showed measurable inhibition of tumor growth evidenced by the lack of increase in tumor size and overall image intensity.

The ability to quantify i.p. tumor growth using luminescent imaging was demonstrated for control and topotecan-treated athymic female mice inoculated i.p. with MCF-7 Luc cells. As shown in Figure 4, the growth of MCF-7 Luc cells in control mice and in topotecan-treated mice was measured over a period of 20 days by serial imaging. Tumor volumes up to 800 000 counts/s were measured in control mice. Figure 5 shows representative imaging results for control and topotecan-treated mice inoculated i.p. with MCF-7 Luc cells. Growth and inhibition of MCF-7 Luc cells i.p. could be quantified in individual mice by serial luminescent imaging without the need to sacrifice animals at each time point.

Discussion

In recent years, luminescent and fluorescent imaging have been explored for pre-clinical *in vivo* drug development studies [31,32,34,36]. We and others have previously reported that luciferase-transfected human tumor xenografts may be useful to study oncogenesis and metastasis [9,13–22]. In particular, luminescent imaging of xenografts makes it possible to study primary tumors and metastasis in deep tissues and distant organs without the need to sacrifice animals at serial time points [31,32,34,36]. Differences between luminescent and

Fig. 3

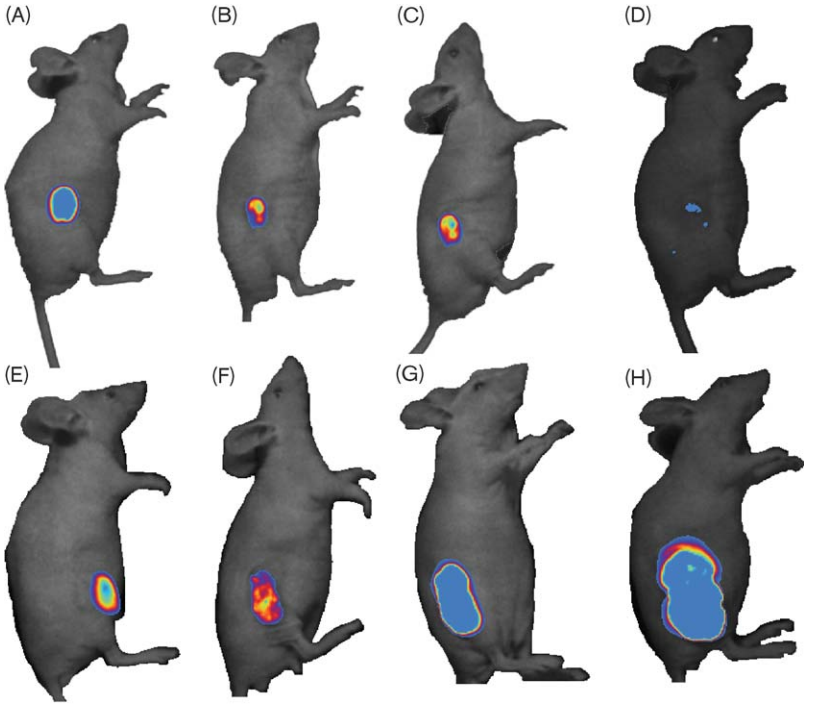

Representative imaging results on days 6, 14, 18 and 27 for mice treated with topotecan (2.5 mg/kg) or PBS on days 7, 11, 15 and 19 after s.c. inoculation of 5×10^6 DU-145 Luc cells. (A–D) Imaging results for a mouse treated with topotecan. (E–H) Imaging results for a control PBS-treated mouse.

Fig. 5

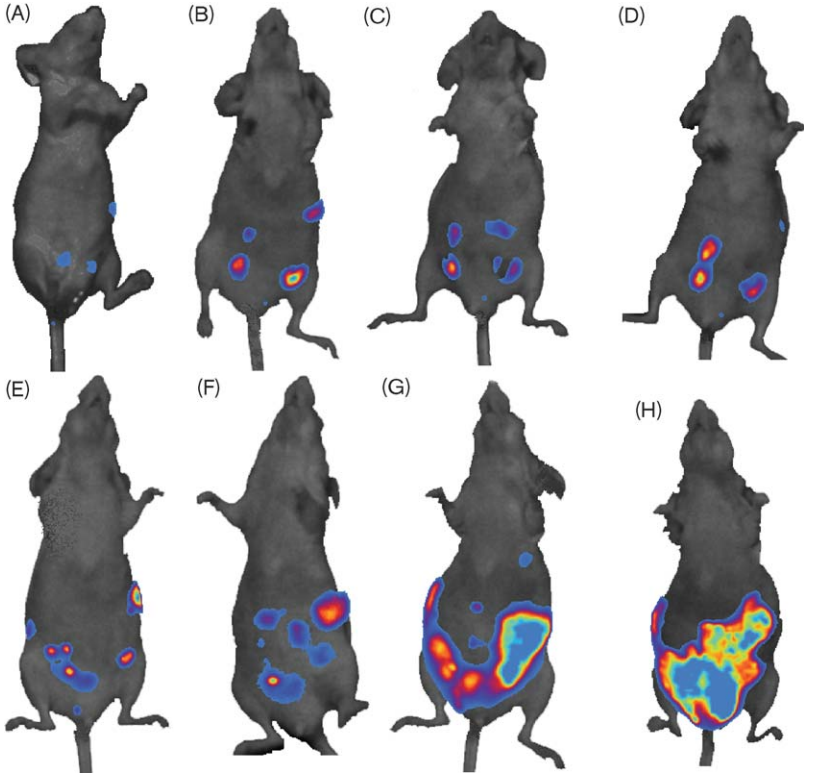

Representative imaging results on days 6, 12, 16 and 20 for mice treated with topotecan (2.5 mg/kg) or PBS on days 9, 13, 17 and 21 after i.p. inoculation of 5×10^6 MCF-7 Luc cells. (A–D) Imaging results for a mouse treated with topotecan. (E–H) Imaging results for a control PBS-treated mouse.

Fig. 4

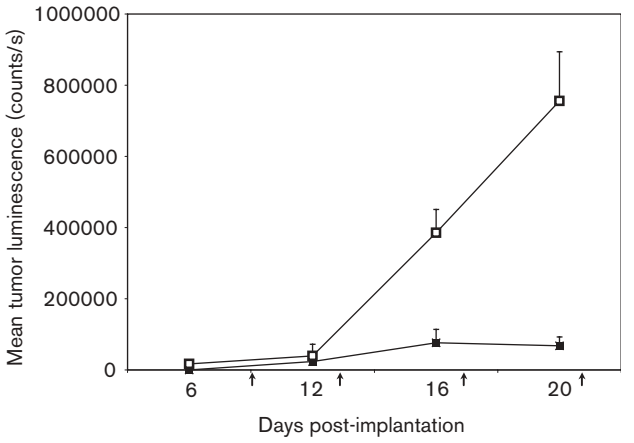

Development of MCF-7 tumors in female athymic *nu/nu* mice after i.p. inoculation of 5×10^6 cells. Mice were treated with PBS or topotecan (2.5 mg/kg) on days 9, 13, 17 and 21 after tumor inoculation as shown by arrows. (□) Mean luminescence of control mice treated with PBS and (■) mean luminescence of experimental mice treated with topotecan.

fluorescent imaging have been demonstrated for detection of deep tissue metastasis [9,34,35].

These studies probe the efficacy of luminescent imaging for testing the activity of chemotherapeutic agents against i.p. and s.c. tumor lesions. It was possible to measure the growth of i.p. and s.c. tumor mass by luminescence. Furthermore, there is good correlation between the traditional method of measuring the growth of s.c. lesions with a caliper and values obtained with luminescent imaging systems. Topotecan alone inhibits the growth of tumor lesions in mice inoculated with the human breast cancer MCF-7 Luc, as has been reported in multidrug resistance studies [47,48]. We also found that it is possible to measure chemotherapeutic drug activity *in vivo* against s.c. and i.p. tumors by luminescent imaging. In this model system, we also observed topotecan activity in mice inoculated with human prostate cancer DU-145 Luc. However, the response to topotecan in humans with prostate cancer has been limited [49–51].

It is of particular interest that some MCF-7 Luc and DU-145 Luc tumors did not completely disappear, but also did not expand appreciably. This suggests that these tumors may be exhibiting some mechanisms of resistance. Luminescent imaging technology allows us to follow, locate and examine these resistant tumors by different methods, including genetic and functional analysis. By examining tumors that have not completely responded to drug therapy we can now explore mechanisms of resistance. This will open up a new avenue of experimentation wherein animals can be exposed to suboptimal doses of chemotherapeutic agents and tumors that are not eliminated can be identified, removed and studied. Studies that should yield relevant data will include *in vitro* chemosensitivity studies comparing tumors that are resistant *in vivo* with parental cell lines, microarray analysis to examine changes in RNA expression associated with resistance, and DNA analysis to identify specific mutations that may have occurred and be associated with the resistant phenotype.

While these studies are potentially important to understanding sensitivity and resistance mechanisms, it is important to consider some limitations of *in vivo* studies not directly associated with the luminescence imaging method. Primarily xenograft models are generally good tools to study the inhibition of tumor growth *in situ*, but a major drawback of these models is their lack of spontaneous metastasis to clinically relevant organs such as lungs, brain and bone marrow [19]. To overcome this limitation, we are currently conducting imaging studies using the luciferase-transfected GI-101A cell line, which more closely resembles clinical disease in humans. This human breast cell line metastasizes spontaneously to the lungs of mice after s.c. implantation and a significant period of growth [52,53]. The GI-101A Luc model system should prove to be particularly useful for studying oncogenesis, metastasis and therapy of breast cancer.

Acknowledgments

The authors thank Mr Howard Izenwasser for assistance with the figures and Ms Kerry Titus for her technical help.

References

1 Mansky PJ. Mistletoe and cancer: controversies and perspectives. *Semin Oncol* 2002; **29**:589–594.
2 Gooderham NJ, Zhu H, Lauber S, Boyce A, Creton S. Molecular and genetic toxicology of 2-amino-1-methyl-6-phenylimidazo[4,5-*b*]pyridine (PhIP). *Mutat Res* 2002; **506/507**:91–99.
3 Moschos SJ, Mantzoros CS. The role of the IFG system in cancer: from basic to clinical studies and clinical applications. *Oncology* 2002; **63**:317–332.
4 Bunn Jr PA, Franklin W. Epidermal growth factor receptor expression, signal pathway, and inhibitors in non-small cell lung cancer. *Semin Oncol* 2002; **29**:38–44.
5 Herber D, Lu QY. Overview of mechanisms of action of lycopene. *Exp Biol Med* 2002; **227**:920–923.
6 Calle EE, Frumkin H, Henley SJ, Savitz DA, Thun MJ. Organochlorines and breast cancer risk. *CA Cancer J Clin* 2002; **52**:301–309.
7 Murillo G, Mehta RG. Cruciferous vegetables and cancer prevention. *Nutr Cancer* 2001; **41**:17–28.
8 Nutting CM, Huddart RA. Retinoids in the prevention of bladder cancer. *Expert Rev Anticancer Ther* 2001; **1**:541–545.
9 Andreotti PE, Caceres G, Zankina R, Dauphinee M. Luminescence applications for chemotherapeutic drug development. *Rec Results Cancer Res* 2003; **161**:3–12.
10 Andreotti PE, Cree IA, Kurbacher CM, Hartmann DM, Linder D, Harel G, *et al.* Chemosensitivity testing of human tumors using a microplate adenosine triphosphate luminescence assay: clinical correlation for cisplatin resistance of ovarian carcinoma. *Cancer Res* 1995; **55**:5276–5282.
11 Caceres G, Dauphinee MJ, Eisle LE, Maccoll R, Mizejewski GJ. Anti-prostate cancer and anti-breast cancer activities of two peptides derived from alpha-fetoprotein. *Anticancer Res* 2002; **22**:2817–2820.
12 Kurbacher CM, Bruckner HW, Andreotti PE, Kurbacher JA, Sass G, Krebs D. *In vitro* activity of titanocenedichloride versus cisplatin in four ovarian

carcinoma cell lines evaluated by a microtiter plate ATP bioluminescence assay. *Anticancer Drugs* 1995; **6**:697–704.
13 Bankert RB, Hess SD, Egilmez NK. SCID mouse models to study human cancer pathogenesis and approaches to therapy: potential, limitations, and future directions. *Front Biosci* 2002; **7**:c44–c62.
14 Malkinson AM. Primary lung tumors in mice as an aid for understanding, preventing, and treating human adenocarcinoma of the lung. *Lung Cancer* 2001; **32**:265–279.
15 Xie K, Wang B, Shi Q, Abbruzzese JL, Xiong Q, Le X. Mouse models of metastatic pancreatic adenocarcinoma. *Int J Pancreatol* 2001; **29**:25–35.
16 Van Etten RA. Pathogenesis and treatment of Ph + leukemia: recent insights from mouse models. *Curr Opin Hematol* 2001; **8**:224–230.
17 Teicher BA. Malignant cells, directors of the malignant process: role of transforming growth factor-beta. *Cancer Metastasis Rev* 2001; **20**:133–143.
18 Hsieh CL, Chung LW. New prospective of prostate cancer gene therapy: molecular targets and animal models. *Crit Rev Eukaryot Gene Expr* 2001; **11**:77–120.
19 Van Weerden WM, Romijin JC. Use of nude mouse xenograft models in prostate cancer research. *Prostate* 2000; **43**:263–271.
20 Bankert RB, Chen FA, Sugiyama Y, Egilmez N. Patient immune response to tumors monitored using SCID mouse models. *Immunol Invest* 2000; **29**:171–176.
21 Hoffman RM. Orthotopic metastatic mouse models for anticancer drug discovery and evaluation: a bridge to the clinic. *Invest New Drugs* 1999; **17**:343–359.
22 Satyamoorthy K, Meier F, Hsu MY, Berking C, Herlyn M. Human xenografts, human skin and skin reconstructs for studies in melanoma development and progression. *Cancer Metastasis Rev* 1999; **18**:401–415.
23 White MRH, Craig FF, Watmore D, McCapra F, Simmonds AC. Applications of the direct imaging of firefly luciferase expression in single intact mammalian cells using charge-coupled device cameras. In: Stanley PE, Kricka LJ (editors): *Bioluminescence and Chemiluminescence Current Status*. Chichester: Wiley; 1990, pp. 357–360.
24 Willard ST, Faught WJ, Frawley LS. Real-time monitoring of estrogen-regulated gene expression in single, living breast cancer cells: a new paradigm for the study of molecular dynamics. *Cancer Res* 1997; **57**:4447–4450.
25 Schuler G, Walenta S, Karbach U, Mueller-Klieser W. A bioluminescence method for high resolution imaging of metabolite concentrations in tumor cell aggregates. In: Stanley PE, Kricka LJ (editors): *Bioluminescence and Chemiluminescence Current Status*. Chichester: Wiley; 1990, pp. 353–356.
26 Contag CH, Contag PR, Mullins JI, Spillman SD, Stevenson DK, Benaron DA. Photonic detection of bacterial pathogens in living hosts. *Mol Microbiol* 1995; **18**:593–603
27 Lipshutz GS, Gruber CA, Cao Y, Hardy J, Contag CH, Gaensler KML. *In utero* delivery of adeno-associated viral vectors: intraperitoneal gene transfer produces long-term expression. *Mol Ther* 2001; **3**:284–292.
28 Francis KP, Joh D, Bellinger-Kawahara C, Hawkinson MJ, Purchio TF, Contag PR. Monitoring bioluminescent *Staphylococcus aureus* infections in living mice using a novel lux ABCDE construct. *Infect Immun* 2000; **68**:3594–3600.
29 Francis KP, Yu J, Bellinger-Kawahara C, Joh D, Hawkinson MJ, Xiao G, *et al.* Visualizing pneumococcal infections in the lungs of live mice using bioluminescent *Streptococcus pneumoniae* transformed with a novel gram-positive lux transposon. *Infect Immun* 2001; **69**:3350–3358.
30 Rocchetta HL, Boylan CJ, Foley JW, Iversen PW, Letourneau DL, McMillian CL, *et al.* Validation of a noninvasive, real-time imaging technology using bioluminescent *Escherichia coli* in the neutropenic mouse thigh model of infection. *Antimicrob Agents Chemother* 2001; **45**:129–137.
31 Edinger M, Sweeney TS, Tucker AA, Olomu AB, Negrin RS, Contag CH. Noninvasive assessment of tumor cell proliferation in animal models. *Neoplasia* 1999; **1**:303–310.
32 Sweeney TJ, Mailander V, Tucker AA, Olomu AB, Zhang W, Cao Y, *et al.* Visualizing the kinetics of tumor-cell clearance in living animals. *Proc Natl Acad Sci* 1999; **96**:12044–12049.
33 Brizel DM, Schroeder T, Scher RL, Walenta S, Clough RW, Dewhirst MW, *et al.* Elevated tumor lactate concentrations predict for an increased risk of metastases in head-and-neck cancer. *Int J Radiat Oncol Biol Phys* 2001; **51**:349–353.
34 Caceres G, Zhu X, Jiao J, Zankina R, Aller A, Andreotti P. imaging of luciferase and GFP transfected human tumors in nude mice. *Luminescence* 2003; in press.
35 Le Pivert PJ, Doulat J, Decatur C, Drogo M, Hartov A, Caceres G. In search of modeling the ice ball kill zone Preliminary results of an experimental study. In: Korpan N (editor): *Theoretical and Experimental Aspects of Cryosurgery*. Vienna: Spring-Verlag; 2003, in press.
36 Contag CH, Jenkins D, Contag P, Negrin R. Use of reporter genes for optical measurements of neoplastic disease *in vivo*. *Neoplasia* 2000; **2**:41–52.
37 Hoffman RM. Green fluorescent protein imaging of tumor growth, metastasis, and angiogenesis in mouse models. *Lancet Oncol* 2002; **3**:545–556.
38 Yang M, Baranov E, Wang J, Jiang P, Wang X, Sun F, *et al.* Direct external imaging of nascent cancer, tumor progression, angiogenesis, and metastasis on internal organs in the fluorescent orthotopic model. *Proc Natl Acad Sci* USA 2002; **99**:3824–3829.
39 Yang M, Hasegawa S, Jian P, Wang X, Tan Y, Chishima T, *et al.* Widespread skeletal metastatic potential of human lung cancer revealed by green fluorescent protein expression. *Cancer Res* 1998; **58**:4217–4221.
40 Chishima T, Miyagi Y, Wang X, Yamaoka H, Shimada H, Moossa AR, *et al.* Cancer invasion and micrometastasis visualized in live tissue by green fluorescent protein expression. *Cancer Res* 1997; **57**:2042–2047.
41 Chishima T, Miyagi Y, Wang X, Baranov E, Tan Y, Shimada H, *et al.* Metastatic patterns of lung cancer visualized live and in process by green fluorescence protein expression. *Clin Exp Metastasis* 1997; **15**:547–552.
42 Adams DJ, Dewhirst MW, Flowers JL, Gamcsik MP, Colvin OM, Manikumar G, *et al.* Camptothecin analogues with enhanced antitumor activity at acidic pH. *Cancer Chemother Pharmacol* 2000; **46**:263–271.
43 Platzer P, Herzog W, Thalhammer T, Hamilton G, Haberl I, Jager W. Formation of a novel topotecan metabolite in the hormone-independent human prostate carcinoma cell lines DU-145 and PC-3. *Anticancer Res* 1998; **18**:2737–2742.
44 Kaufmann SH, Peereboom D, Buckwalter CA, Svigen PA, Grochow LB, Donehower RC, *et al.* Cytotoxic effects of topotecan combined with various anticancer agents in human cancer cell lines. *J Natl Cancer Inst* 1996; **88**:734–741.
45 Husain K, Mohler JL, Seigler F, Besterman JM. Elevation of topoisomerase I messenger RNA, protein and catalytic activity in human tumors: demonstration of tumor-type specificity and implications for cancer chemotherapy. *Cancer Res* 1994; **54**:539–546.
46 Schwartz GN, Teicher BA, Eder Jr JP, Korbut T, Holden SA, Ara G, *et al.* Modulation of antitumor alkylating agents by novobiocin, topotecan, and lonidamine. *Cancer Chemother Pharmacol* 1993; **32**:455–462.
47 Vanhoefer U, Muller MR, Hilger RA, Lindtner B, Klaassen U, Schleucher N, *et al.* Reversal of MDR1-associated resistance to topotecan by PAK-200S, a new dihydropyridine analogue, in human cancer cell lines. *Br J Cancer* 1999; **81**:1304–1310.
48 Litman T, Brangi M, Hudson E, Fetsch P, Abati A, Ross DD, *et al.* The multidrug-resistant phenotype associated with overexpression of the new ABC half-transporter, MXR (ABCG2). *J Cell Sci* 2000; **113**:2011–2021.
49 Klein CE, Tangen CM, Braun TJ, Hussain MH, Peereboom DM, Nichols CR, *et al.* SWOG-9510: evaluation of topotecan in hormone refractory prostate cancer: a Southwest Oncology Group study. *Prostate* 2002; **52**:264–268.
50 Hudes GR, Kosierowski R, Greenberg R, Ramsey HE, Fox SC, Ozols RF, *et al.* Phase II study of topotecan in metastatic hormone-refractory prostate cancer. *Invest New Drugs* 1995; **13**:235–240.
51 Heron J-F. Topotecan: an oncologist's view. *The Oncologist* 1998; **3**:390–402.
52 Hoelting T, Goretzki PE, Duh Q-Y. Follicular thyroid cancer cells: a model of metastatic tumor *in vitro* [Review]. *Oncol Rep* 2001; **8**:3–8.
53 Hurst J, Maniar N, Tombarkiewicz J, Lucas F, Roberson C, Steplewski Z, *et al.* A novel model of a metastatic human breast tumor xenograft line. *Br J Cancer* 1993; **68**:274–276.